LASER PULSE ANALYSIS FOR RECONSTRUCTION AND CLASSIFICATION OF URBAN OBJECTS

B. Jutzi, U. Stilla

FGAN-FOM Research Institute for Optronics and Pattern Recognition
76275 Ettlingen, Germany
{jutzi,stilla}@fom.fgan.de

Commission III

KEY WORDS: Object recognition, Urban areas, Waveform analysis, Pulsed laser radar.

ABSTRACT:

Current pulsed laser radar systems for topographic applications are based on time-of-flight ranging techniques to determine the range of the illuminated object. The signal analysis to determine the time-of-flight typically operates with analogous threshold detection. In this paper we describe investigations for digital recording of received laser pulses and a detailed analysis of the pulse waveform. Recording the complete signal is advantageous because it allows processing depending on different tasks, respecting intermediate results, and considering neighbourhood relations. Two different techniques for measurement of time resolved laser pulses are presented. An experimental system for a fast recording of signals was constructed. For principal investigations a test board with urban materials was measured by single photon detection technique and visualized by a data cube. Based on these spatio-temporal data, different features are extracted and depicted by grey value images to describe macro, meso, and micro structures. Measurements were carried out with partial occlusion of the test board by vegetation. Multiple reflections are counted by processing the data cube using a spatio-temporal filter and peak detector. Initial results of object segmentation are shown.

1. INTRODUCTION

The automatic generation of 3-d models for a description of man-made objects, like buildings, is of great interest. In photogrammetry a spatial surface is classically determined by triangulation of corresponding image points from two or more pictures of the surface. The points are manually searched or automatically detected by analyzing image structures (e.g. stereo correlation techniques). Besides this indirect measurement using object characteristics which depend on natural illumination, active laser radar systems allow a direct and illumination-independent measurement of the range. The laser radar captures the range information of 3-d objects in a fast, contactless and accurate way. In future applications the reliability of measurements and the capability for object recognition could be increased by analyzing object features.

Current pulsed laser radar systems for topographic applications are based on time-of-flight ranging techniques to determine the range of the illuminated object. Overviews are given in Baltsavias (1999), Huising & Pereira (1998) and Wehr & Lohr (1999). The time-of-flight is measured by the elapsed time between the emitted and backscattered laser pulses. The signal analysis to determine the elapsed time typically operates with analogous threshold detection (e.g. peak detection, leading edge detection, constant fraction detection). Currently first pulse as well as last pulse exploitation are used for different applications (urban planning, forestry surveying, power line monitoring) to capture a three-dimensional scene (digital terrain model, digital surface model, city model).

While first pulse registration is the optimum choice when surveying the top of objects (e.g. canopy), last pulse registration should be chosen if the final elevation model should describe the ground surface. Figure 1a shows a section of an image taken in first pulse mode in October. The foliage of the trees is visible. Figure 1b was taken in last pulse mode in January. The branches and foliage are not visible and the building areas are smaller than in Figure 1a. Due to multiple pulse reflection at the boundary of the buildings and the processing by first or last pulse mode, building areas dilate or erode. Similar results can be achieved by corresponding rank value filters. In some areas no response could be received due to the weak reflectivity of snow and ice at the operating wavelength of 1,55 μm.

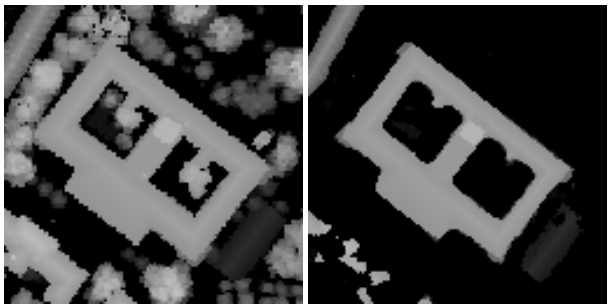

a b

Figure 1. Sections of elevation images of an urban scene (Test area Karlsruhe, Germany). a) first pulse mode, b) last pulse mode.

Beside the first or last pulse exploitation the complete signal waveform in between might be of interest, because it includes the backscattering characteristic of the illuminated field. This enhanced information is helpful to explore the vegetation concerning the bio mass, foliage or density (e.g. trees, bushes, ground). Several groups are conducting research on natural objects. NASA has developed a prototype of a Laser Vegetation Imaging Sensor (LVIS) for recording the waveform to determine the vertical density profiles in forests (Blair *et al.*, 1999). The spaceborne Geoscience Laser Altimeter System

(GLAS) determines distance to the Earth's surface, and a profile of the vertical distribution of clouds and aerosols. In some applications (e.g. observation of climate changes), clouds are objects of interest. In other application clouds are considered as obstacles, which limit the visibility of the illuminated object.

In addition to range, some systems deliver a reflectance value derived from the intensity of the backscattered laser light. This reflectance value can be used for separating segments of artificial objects from vegetation (Hug & Wehr, 1997; Maas, 2001).

In this paper we describe investigations for a detailed analysis of laser pulses. In Section 2 different techniques for measurement of time resolved laser pulses are discussed. The experimental system for a fast recording of signals is described in Section 3. In Section 4 the performed experiments are explained and the measured data are depicted. The determined features of the data are presented in Section 5. First steps for a segmentation of objects are shown in Section 6.

2. MEASUREMENT TECHNIQUES

2.1 Laser radar systems

Depending on the application, laser radar systems can be designed in different ways (Kamermann, 1993). They may differ in techniques concerning e.g. the modulation, detection, or measurement.

Concerning the modulation techniques laser systems can be split in continuous wave (cw) laser or pulsed laser. For applications in remote sensing the pulsed laser with the higher power density compared to cw laser is of advantage, because it allows for operating at long ranges. In this work we focus on pulsed laser systems.

Detection techniques can be divided in coherent detection and direct detection (Jelalian, 1992). Coherent detection considers the wave front of the received signal compared to a reference signal emitted from a cw laser. In direct detection laser systems the received optical energy is focused onto a photosensitive element that generates a value that depends on the optical power. The possibility to detect multiple or single photons is described in the next section.

Measurement techniques for range determination can be distinguished by the exploited signal properties such as phase, amplitude, frequency, polarization, time, or any combination of them. We are interested in measuring and analyzing the received pulse waveform, i.e. the dependence of the intensity over time.

2.2 Recording the signal waveform

Two detection techniques seem to be appropriate to record the temporal characteristic of the backscattered signal: multi photon detection (Figure 2) and single photon detection (Figure 3).

2.2.1 Multi photon detection: The classical measurement technique for direct detection operates with a photodiode (usually PIN- or avalanche photodiode). The photodiode generates an electrical signal (voltage or current) that is directly proportional to the optical power of the incident light (multi photon). For a detailed analysis of the signal waveform a digitizing receiver unit is essential. Analyzing the signal waveform of the emitted short duration laser pulse with only a few nanoseconds pulse width requires a receiver unit processing the data with a bandwidth of some GHz and an appropriate sampling rate. Increasing bandwidth results in decreasing sensitivity of the photodiode which can be compensated by increasing power of the emitting laser source. Figure 4a shows a pulse digitized by 5 GSample/s.

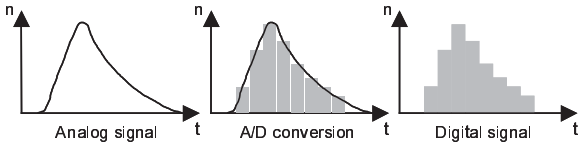

Figure 2. Digital recording of the signal waveform with multi photon detection

2.2.2 Single photon detection: The integration of the incoming radiation by multi photon detection can be seen as collecting a countable number of photons for a limited observation time of one pulse. Let us assume a stationary scene and a stationary sensor platform. In this case the statistical properties of the laser radiation do not change with the time and time-average quantities are equal to the ensemble quantities. Under these assumptions the radiation ensembles are stationary and ergodic (Papoulis, 1984; Troup, 1972). This means that counting single photon events with their time-of-flight into time bins of a histogram is closely related to integration of multi photons over the time (Alexander, 1997; Gagliardi & Karp, 1976; Loudon, 2000). For receiving the temporal waveform of the pulse, a histogram of the photon arrivals over time has to be measured.

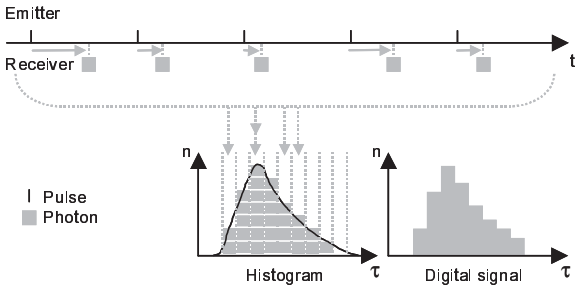

Figure 3. Digital recording of the signal waveform with single photon detection

Many pulses are necessary to obtain a signal waveform with single photon detection. The quality of the sampled signal waveform depends on the number of photon counts. Figure 4b shows a pulse plotted from a histogram containing the time-of-flight measurements from 6135 photons distributed in 25 bins (bin width ≙ 40 ps).

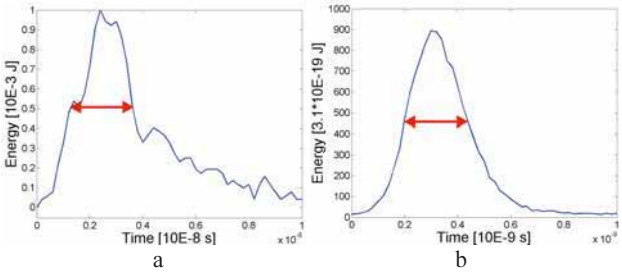

Figure 4. Examples for pulses backscattered from a diffuse surface. a) multi photon detection (FWHM = 2,3 ns), b) single photon detection (FWHM = 0,3 ns)

The full-width-half-maximum (FWHM) of the pulse in Figure 4a is about eight times of the pulse in Figure 4b. For experimental investigations on the signal waveform a short duration laser pulse is helpful. In contrast to previous work (Jutzi *et al.*, 2003), this paper focusses on single photon detection.

3. EXPERIMENTAL SETUP

An experimental setup was constructed for exploring the capabilities of recognizing urban objects using a laser system. For principle investigations of the influence of different object properties (e.g. geometry, material) on the signal waveform a pulsed laser system with single photon detection is used. In contrast to single photon approaches which exploit only a few photons for a range measurement (Ho *et al.*, 1999; Priedhorsky *et al.*, 1996), we are interested in receiving more photons to obtain a detailed distribution for analyzing the signal waveform.

The measurements are carried out indoors by an experimental setup which consists of a laser system and a target with different urban materials.

3.1 Laser system

The laser system consists of three main components: (i) an emitter unit, (ii) a receiver unit, and (iii) a motion control unit.

We use a short duration laser pulse system with a high repetition rate. The pulsed diode laser operates at a wavelength of 640 nm. The average power of the laser is up to 30 mW and pulse duration with less than 70 ps FWHM. The user-selectable repetition rate is from 2.5 MHz to 80 MHz and allows an unambiguous range measurement up to 60 m. This maximum unambiguous range is given by the slowest repetition rate and the time-of-flight of the laser pulse. The receiver unit consists of a photomultiplier tube which detects up to 3 million single photon events per second and a device which exploits the received data and computes a histogram. The receiver unit limits the temporal resolution to a minimum pulse width of 300 ps (FWHM) and the minimum recording time is 1 ms per measurement of the signal waveform. For the 2-d scan, a mirror, two linear actuators, and a motion controller are used to redirect the laser beam. The angle accuracy of the motion control unit is approximately 20 µrad. All units are synchronized and controlled with a PC.

3.2 Targets

Depending on the application different properties of urban surfaces can be sensed by a laser system. According to the size of the focused surface geometry in relation to the beam (footprint and wavelength) we divide surface structures into macro, meso, and micro structures (Figure 5).

3.2.1 Macro Structure: We interpret macro structures as structures which are much more extended than the beam footprint d. Laser range measurements taken by a scan allow a reconstruction of large object structures like different roof shapes (e.g. flat roof, gabled roof, hip roof, etc.). The scan is typically spaced greater than the spatial beam width for aerial survey purposes.

3.2.2 Meso Structure: We interpret meso structures as structures which are much less extended than the beam footprint d and much greater than the wavelength λ. Different elevated object surfaces within the beam corridor lead to a mixture of different range values. This may be caused by small elevated objects (e.g. a chimney), a slanted plane, or vegetation like branches or leaves of a tree.

3.2.3 Micro Structure: We interpret micro structures as structures which are less extended than the wavelength λ. Depending on the roughness the irradiance is more or less reflected. A single measurement of the backscattered beam intensity (amplitude) gives information about the roughness of the surface and the material. Small roughness results in specular reflectance and large roughness in diffuse reflectance.

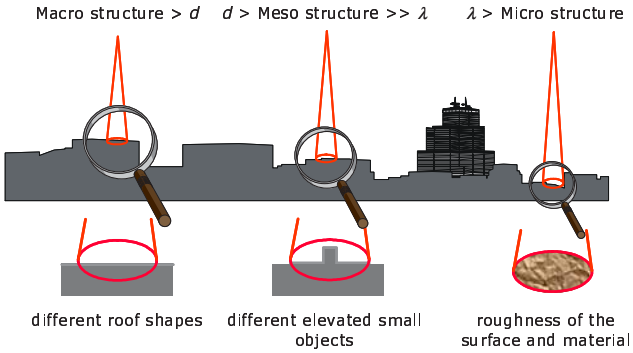

Figure 5. Different levels of details sensed by a laser system

4. EXPERIMENTS

4.1 Test board

According to the focused structure, class relevant signal features have to be examined. For this purpose a test board was designed which consist of different urban materials (Figure 6): corrugated iron (left above), pebbles (background), slanted slate plate (right above), and flat roof tile (right below). The materials have different backscattering characteristics and are mounted in different ranges.

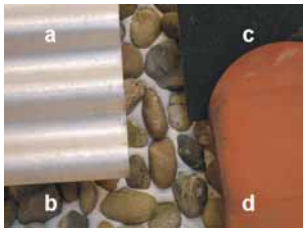

Figure 6. Test board with different urban materials.
a) corrugated iron, b) pebbles, c) slanted slate plate,
d) flat roof tile

4.2 Scan

The test board was illuminated by a pulsed laser with a wavelength of approximately 640 nm and a footprint of approximately 5 mm (beam divergence 1 mrad). The time-of-flight distribution of the received photon events (cf. Figure 4a) was recorded with a temporal resolution of 40 ps and 4096 bins which results in a range interval of approximately 25 m and a range resolution of 6 mm. A section of the test board (approximately 0.4 m x 0.3 m) was scanned by 128 columns steps and 128 rows steps.

4.3 Visualization

Displaying the time-of-flight as distance the data set can be seen as a spatial distribution. Assuming Cartesian coordinates the spatial distribution may be visualized by a cube (x,y,t). Figure 7 shows a section of the cube (Δt=32 bins), where the grey values correspond to the intensity of the signal (number of photons). The corrugated iron is on the left side and the roof tile on the right side of the cross range plane. The pebbles are inside the selected cube. The temporal dependency of the uppermost row and the right column on the signal is depicted on top plane and right plane. For visualization purposes the dynamic level was adjusted.

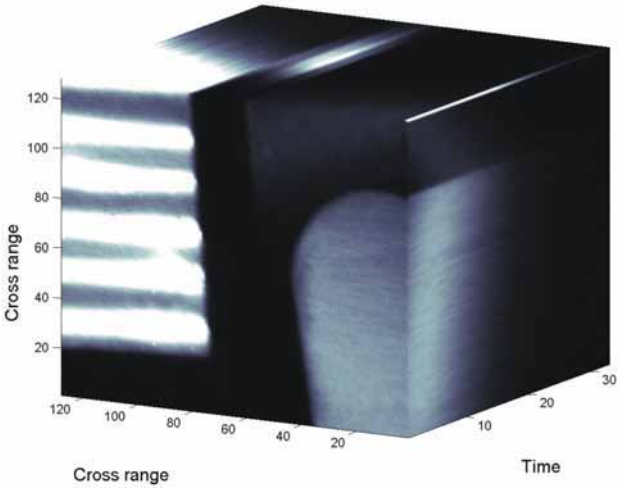

Figure 7. Visualization of time-dependent intensity values of the scanned test board

5. ANALYSIS

5.1 Pulse analysis for macro structures

For measuring macro structures with extended surfaces we assume to receive single pulses, i.e. we neglect the boundaries (discontinuities) within the footprint. Storing the data cube opens the possibility of using different ranging techniques to exploit the received pulses *s(t)*, e.g. peak detection, leading edge detection, constant fraction detection, average time value detection (Figure 8).

5.1.1 Peak detection: The range value is determined by the maximum pulse amplitude, where the highest reflectance is expected (Figure 8a). Regional spikes on the pulse waveform strongly effect the range detection. We processed the range values without temporal filter. For noisy signals, a filter is recommended to determine the global maxima.

5.1.2 Leading edge detection: The threshold crossing by the exceeding pulse waveform determines the range (Figure 8b). The threshold value can be a predefined fixed value, but then the ranging detection strongly depends on the pulse waveform, amplitude, and width of the pulse. We used half of the maximum amplitude of the pulse for a threshold with linear interpolation for range determination. This ranging detection gives the shortest range values.

5.1.3 Constant fraction detection (CFD): The pulse waveform *s(t)* is inverted and delayed by a fixed time τ and added to the original pulse (Figure 8c). The combined signal *c(t)* give a constant fraction signal with a zero crossing point, which is insensitive to the pulse amplitude, but depends on the pulse waveform and width (Kamermann, 1993). We used 300 ps (FWHM) for delay time τ.

$$t_{CFD} \Leftrightarrow c(t) = s(t) - s(t+\tau) = \begin{cases} t_{CFD} & if \quad c(t) = 0 \\ 0 & if \quad c(t) \neq 0 \end{cases} \tag{1}$$

5.1.4 Average time value detection: The temporal centre of gravity of the pulse waveform is determined (Figure 8d). It delivers good results for small noise, various pulse amplitudes and pulse widths. The asymmetric pulse shape results in range detection, which is slightly behind the range value detected with the peak detection.

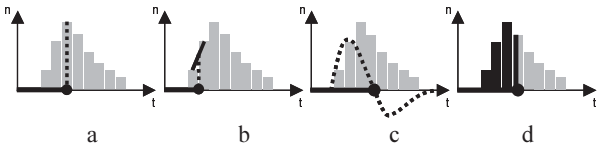

Figure 8. Ranging techniques. a) peak detection, b) leading edge detection, c) constant fraction detection, d) average time value detection

The range images processed with the different ranging techniques are depicted in Figure 9. The range is visualized by grey values whereas the slanted slate plate (right above) shows increasing values and the corrugated iron (left) shows wavy grey values. For visualization purposes the temporal jitter of the different techniques is eliminated by adjusting the average value of the complete range images to each other. The range resolution with peak detection in Figure 9a appears coarser than in the other Figures. The smoothest range resolution is is processed with average time value detection with Figure 9d.

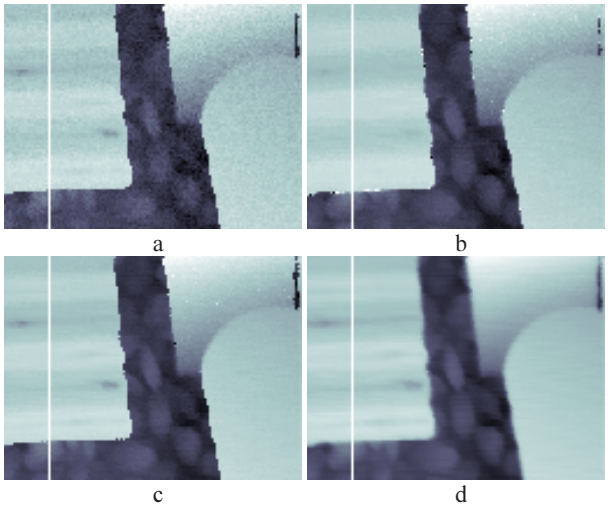

Figure 9. Range images. a) peak detection, b) leading edge detection, c) constant fraction detection, d) average time value detection

In Figure 10a range profiles taken from range images in Figure 9 (see vertical line) are depicted. The leading edge and the constant fraction detection show small systematic ranging errors for different pulse widths. Peak detection appears noisy. Discontinuities in the waveform are a general problem for all ranging techniques. Depending on the signal quality, a spatio-temporal filter might be helpful to increase the precision of range detection.

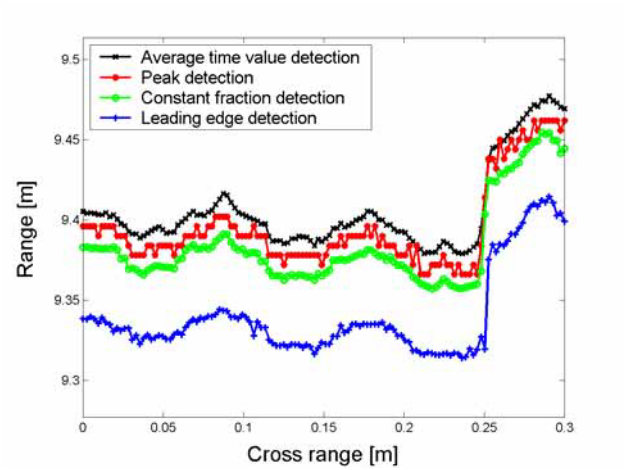

Figure 10. Range profiles

5.2 Pulse analysis for meso structures

Different elevated object surfaces within the beam corridor lead to a mixture of different range values. A plane which is slanted in viewing direction shows different range values within the footprint. This range interval which is given by the size of the footprint and the orientation of the plane leads to a temporal spread of the pulse (Figure 11b). A deformation of the pulse waveform can also be caused by perpendicularly oriented plane surfaces shifted by a small step in viewing direction (Figure 11c). A large step leads to two separate pulses (Figure 11d). Several surfaces with different range within the beam result in multiple pulses. These examples are simplified and not exhaustive.

The increased pulse width indicates an uneven, slanted or small stepped surface. A peak detector is used to separate a single pulse from multiple pulses in the data cube. The pulse width is calculated as standard deviation from the time-of-flight values of the photons. In Figure 12 the pulse widths of maximum pulses are depicted by different grey values. The slanted slate plate (top right) and the contours of the pebbles (centre) appear brighter than the surroundings.

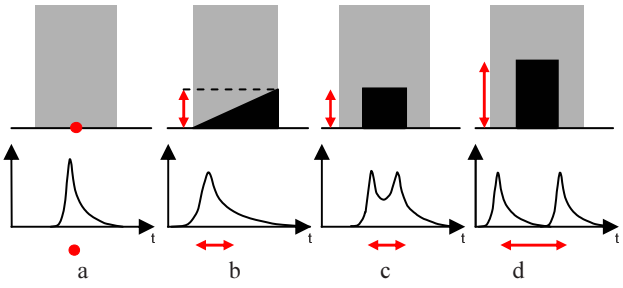

Figure 11. Surface and pulse waveform. a) flat surface, b) slanted surface, c) small step, d) large step

Figure 12. Pulse width image (Angle of the slate plate: 33°).

5.3 Pulse analysis for micro structures

Depending on the material and the surface roughness (micro structure) objects show different reflectance properties. The amount of backscattered photons varies with these properties. The received maximal pulse amplitude and pulse power P

$$P = \frac{1}{2T}\int_{-T}^{T} s^2(t)dt \qquad (2)$$

can be used to discriminate different materials. Figure 13 depicts the pulse power visualized by different grey values. The horizontally oriented areas of the corrugated iron (left) shine bright caused by specular reflectance. The slate plate (top right) appears black caused by the strong absorption.

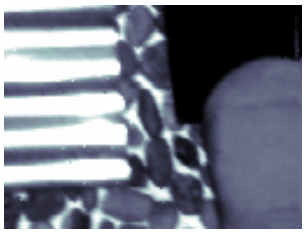

Figure 13. Pulse power image (Gamma corrected)

6. MULTIPLE PULSES

Both first pulse and last pulse detection is used for photogrammetric applications which allows to consider or neglect the presence of vegetation (see Figure 1). In general, from vegetation a various number of pulse reflections can be expected depending on the density and structure. The captured data cube opens the possibility to analyze the data concerning multiple pulses. This might be of interest for discriminating different types of vegetation. Multiple reflection can also be observed for urban structures which are smaller than the footprint (e.g. power lines).

A scene containing vegetation which partly occludes the test board is shown in Figure 14a. Figure 14b depicts the temporal signal waveform of a single measurement. The multiple pulses were caused by branches in different ranges within the beam. Multiple reflections are counted by a peak detector. Figure 14c shows the number of counted pulses by different grey values. The dark areas result from the test board which reflects background as a single pulse. The branches of the foreground cause additional pulses and appear brighter. More than two pulses can be observed at the crossing of branches.

Due to the noise the measured signals were filtered in the data cube by a spatio-temporal Gaussian implement by a 3x3x3 filter. The result of a peak detection is visualized by a 3-d view in Figure 15. A simple segmentation was performed by a threshold operation on the range to separate the branches against the test board.

7. CONCLUSION

The recording of the signal waveform has different advantages for the analysis:

- The recorded data cube of the received signals allows exploiting different features without selecting a special feature in advance.

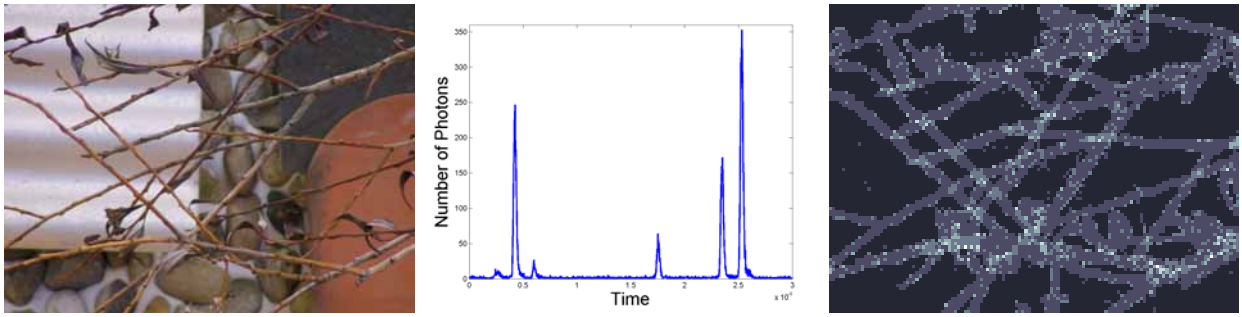

a b c

Figure 14. Multiple pulses. a) vegetation (branches) in front of the test board, b) signal waveform of a single measurement (Number of pulses: 6), c) number of pulses visualized by different grey values

- For processing the data cube an adaptive threshold operation is possible.
- Object recognition from laser data often requires further image processing steps like filtering or segmentation. Instead of exploiting neighbourhood relations within the images, the data cube opens the possibility of a spatio-temporal filtering or segmentation.

For single photon detection we assumed a stationary scene and sensor platform. In our experiments the acquisition time for recording a received pulse by single photon counting and by using a low power laser was about 100 ms. Other authors, e.g. (Pellegrini et al., 2000), carried out a range measurement in 10 ms. The experimental system we used is limited to an acquisition time of 1 ms. Applications using an airborne system require a shorter acquisition time.

The experiments we carried out are general investigations for a laser system which operates with multi photon detection. Future work focuses on a fast digitizing acquisition of single laser pulses with multi photon detection and the analysis of the received signal.

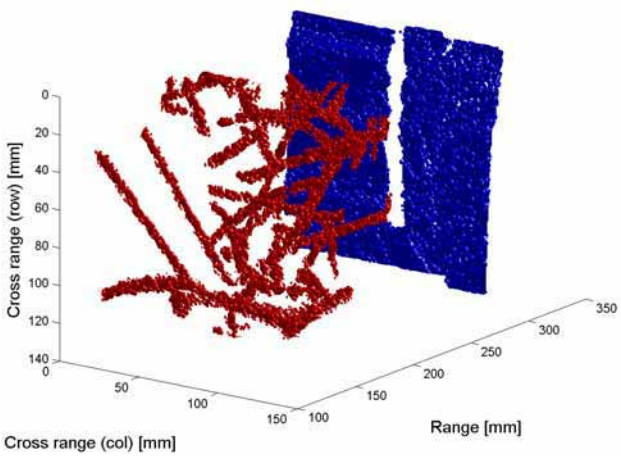

Figure 15. 3-d visualization of segmented objects (branches and test board)

REFERENCES

Alexander SB (1997) Optical Communication Receiver Design. In: SPIE Tutorial Texts in Optical Engineering, vol. TT22, Washington, Bellingham: SPIE

Baltsavias EP (1999) Airbornelaser scanning: existing systems and firms and other resources. ISPRS Journal of Photogrammetry & Remote Sensing 54: 164-198

Blair JB, Rabine DL, Hofton MA (1999) The Laser Vegetation Imaging Sensor (LVIS): A medium-altitude, digitization-only, airborne laser altimeter for mapping vegetation and topography. ISPRS Journal of Photogrammetry & Remote Sensing 56: 112-122

Gagliardi RM, Karp S (1976) Noncoherent (Direct) Detection. Optical Communications. New York: John Wiley & Sons

Ho C, Albright KL, Bird AW, Bradley J, Casperson DE, Hindman M, Priedhorsky WC, Scarlett WR, Smith RC, Theiler J, Wilson KS, (1999) Demonstration of Literal Three-Dimensional Imaging. Applied Optics 38: 1833-1840

Hug C, Wehr A (1997) Detecting and identifying topographic objects in laser altimeter data. ISPRS, International Archives of Photogrammetry & Remote Sensing, Vol. 32, Part 3-4W2: 19-26.

Huising EJ, Gomes Pereira LM (1998) Errors and accuracy estimes of laser data acquired by various laser scanning systems for topographic applications. ISPRS Journal of Photogrammetry & Remote Sensing 53: 245-261

Jelalian AW (1992) Laser Radar systems. Norwood, MA, Boston: Artech House

Jutzi B, Eberle B, Stilla U (2003) Estimation and measurement of backscattered signals from pulsed laser radar. In: Serpico SB (ed) Image and Signal Processing for Remote Sensing VIII, SPIE Proc. Vol. 4885: 256-267

Kamermann GW (1993) Laser Radar. In: Fox CS (ed) Active Electro-Optical Systems, The Infrared & Electro-Optical Systems Handbook. Michigan: SPIE Optical Engineering Press

Loudon R (2000) The Quantum Theory of Light. Oxford: Oxford University Press

Maas HG (2001) The suitability of airborne laser scanner data for automatic 3D object reconstruction. In: Baltsavias EP, Gruen A, Van Gool L (eds) Automatic Extraction of Man-Made Objects From Aerial and Space Images (III), Lisse: Balkema

Papoulis A (1984) Probability, Random Variables, and Stochastic Processes. Tokyo: McGraw-Hill

Pellegrini S, Buller GS, Smith JM, Wallace AM, Cova S (2000) Laser-based distance measurement using picosecond resolution time-correlated single-photon counting. Measurement Science and Technology 11: 712-716

Priedhorsky WC, Smith RC, Ho C (1996) Laser ranging and mapping with a photon-counting detector. Applied Optics 35: 441-452

Troup GJ (1972) Photon Counting and Photon Statistics. In: Sanders JH, Stenholm S (eds) Progress in Quantum Electronics. vol. 2 part 1, Oxford: Pergamon

Wehr A, Lohr U (1999) Airborne laser scanning – an introduction and overview. ISPRS Journal of Photogrammetry & Remote Sensing 54: 68-82